Article

Cell Reports

BRCA1 Directs the Repair Pathway to Homologous Recombination by Promoting 53BP1 Dephosphorylation

Graphical Abstract

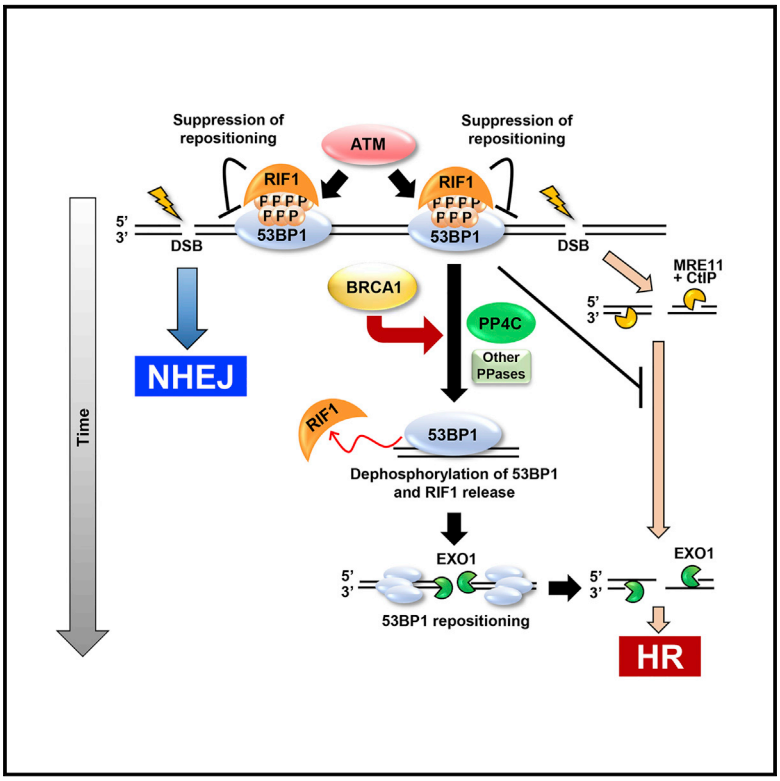

Highlights

- 53BP1 is phosphorylated by ATM in S/G_2, followed by transient RIF1 recruitment
- Inhibiting resection sustains p53BP1-RIF1 interaction
- BRCA1 promotes 53BP1 dephosphorylation and RIF1 release
- PP4C participates in 53BP1 dephosphorylation, promoting RIF1 release and resection

Authors

Mayu Isono, Atsuko Niimi, Takahiro Oike, ..., Shinichiro Nakada, Takashi Nakano, Atsushi Shibata

Correspondence

shibata.at@gunma-u.ac.jp

In Brief

Following induction of DNA double-strand break, a pro-end-joining environment is created in G_2 by transient 53BP1 phosphorylation and RIF1 recruitment. Here, Isono et al. show that, if timely repair does not ensue, BRCA1 promotes 53BP1 dephosphorylation and RIF1 release, favoring repair by homologous recombination.

Isono et al., 2017, Cell Reports *18*, 520–532
January 10, 2017 © 2017 The Author(s).
http://dx.doi.org/10.1016/j.celrep.2016.12.042

OPEN ACCESS
CellPress

Cell Reports
Article

BRCA1 Directs the Repair Pathway to Homologous Recombination by Promoting 53BP1 Dephosphorylation

Mayu Isono,[1,2] Atsuko Niimi,[3] Takahiro Oike,[4] Yoshihiko Hagiwara,[1,4] Hiro Sato,[4] Ryota Sekine,[1] Yukari Yoshida,[2] Shin-Ya Isobe,[5] Chikashi Obuse,[5] Ryotaro Nishi,[6] Elena Petricci,[7] Shinichiro Nakada,[8] Takashi Nakano,[2,3,4] and Atsushi Shibata[1,9,*]

[1]Advanced Scientific Research Leaders Development Unit, Gunma University, Maebashi, Gunma 371-8511, Japan
[2]Gunma University Heavy Ion Medical Center, Gunma University, Maebashi, Gunma 371-8511, Japan
[3]Gunma University Initiative for Advanced Research, Gunma University, Maebashi, Gunma 371-8511, Japan
[4]Department of Radiation Oncology, Gunma University, Maebashi, Gunma 371-8511, Japan
[5]Graduate School of Life Science, Hokkaido University, Sapporo, Hokkaido 060-0810, Japan
[6]Department of Biomedical Sciences, College of Life Sciences, Ritsumeikan University, Kusatsu, Shiga 525-8577, Japan
[7]Department of Biotechnology, Chemistry, and Pharmacy, Università degli Studi di Siena, 53100 Siena, Italy
[8]Department of Bioregulation and Cellular Response, Graduate School of Medicine, Osaka University, Suita, Osaka 565-0871, Japan
[9]Lead Contact
*Correspondence: shibata.at@gunma-u.ac.jp
http://dx.doi.org/10.1016/j.celrep.2016.12.042

SUMMARY

BRCA1 promotes homologous recombination (HR) by activating DNA-end resection. By contrast, 53BP1 forms a barrier that inhibits DNA-end resection. Here, we show that BRCA1 promotes DNA-end resection by relieving the 53BP1-dependent barrier. We show that 53BP1 is phosphorylated by ATM in S/G_2 phase, promoting RIF1 recruitment, which inhibits resection. 53BP1 is promptly dephosphorylated and RIF1 released, despite remaining unrepaired DNA double-strand breaks (DSBs). When resection is impaired by CtIP/MRE11 endonuclease inhibition, 53BP1 phosphorylation and RIF1 are sustained due to ongoing ATM signaling. BRCA1 depletion also sustains 53BP1 phosphorylation and RIF1 recruitment. We identify the phosphatase PP4C as having a major role in 53BP1 dephosphorylation and RIF1 release. BRCA1 or PP4C depletion impairs 53BP1 repositioning, EXO1 recruitment, and HR progression. 53BP1 or RIF1 depletion restores resection, RAD51 loading, and HR in PP4C-depleted cells. Our findings suggest that BRCA1 promotes PP4C-dependent 53BP1 dephosphorylation and RIF1 release, directing repair toward HR.

INTRODUCTION

DNA double-strand breaks (DSBs) represent the most toxic DNA lesion, which, if unrepaired, causes cell death and triggers genomic instability (Jeggo et al., 2011). DSBs are repaired by two major pathways: non-homologous end joining (NHEJ) and homologous recombination (HR). NHEJ occurs throughout the cell cycle in mammalian cells, whereas HR repairs DSBs in S/G_2 phase in a CDK-dependent manner (Chapman et al., 2012b). The DNA-end structure of DSBs is also a critical factor in determining pathway choice (Shibata et al., 2011). One-ended DSBs at stalled/collapsed replication forks are the preferred substrate for HR (Arnaudeau et al., 2001). Despite a pro-HR environment in S/G_2, current models suggest that Ku70/80 heterodimers bind rapidly to DSBs, allowing NHEJ to make the first attempt at repair (Chanut et al., 2016; Chapman et al., 2012b; Shibata et al., 2011, 2014). However, if NHEJ does not ensue, repair switches to HR. This switch is triggered by CtIP-dependent stimulation of MRE11 endonuclease activity (Sartori et al., 2007; Shibata et al., 2014), which makes an initial single-strand (ss) nick 5′ to the DNA end (Garcia et al., 2011; Shibata et al., 2014). Subsequently, exonucleases such as MRE11, EXD2, and EXO1 expand resection by digesting DNA bidirectionally to produce a sufficient length of ssDNA (Broderick et al., 2016; Garcia et al., 2011). Following DNA-end resection, ssDNA is coated by replication protein A (RPA), which is replaced by RAD51 to facilitate homology searching and the subsequent steps of HR.

BRCA1 plays multiple roles that include controlling DNA repair, signaling, chromatin organization, and transcription (Huen et al., 2010). Among these functions, its role in HR is critically important for maintaining genomic stability and suppressing tumorigenesis (Venkitaraman, 2004). BRCA1 promotes HR by activating DNA-end resection (Schlegel et al., 2006). In contrast, 53BP1, a key player in DNA repair and signaling, forms a barrier that prevents excessive resection (Panier and Boulton, 2014). Importantly, an antagonistic relationship between BRCA1 and 53BP1 has been described; embryonic lethality, tumor predisposition, and HR defects in BRCA1-defective cells are restored by depletion of 53BP1 (Bouwman et al., 2010; Bunting et al., 2010). Furthermore, 53BP1 relocates to the foci periphery and vacates the central core as HR ensues in a BRCA1-dependent manner (Chapman

This is an open access article under the CC BY-NC-ND license (http://creativecommons.org/licenses/by-nc-nd/4.0/).

et al., 2012a; Kakarougkas et al., 2013). RPA forms foci that reflect active resection at the site of DSBs. RPA foci form following 53BP1 repositioning and localize to the center of enlarged 53BP1 foci (Kakarougkas et al., 2013). This suggests that resection progresses following 53BP1 repositioning. Thus, the current model is that the major role of BRCA1 is to overcome the barrier against DNA-end resection posed by 53BP1.

Multiple Ser/Thr-Gln (S/T-Q) sites in 53BP1 are phosphorylated by the ataxia-telangiectasia mutated (ATM) kinase in response to DNA damage. Phosphorylation of 53BP1 recruits RIF1 and PTIP (Callen et al., 2013; Chapman et al., 2013; Escribano-Díaz et al., 2013; Feng et al., 2013; Zimmermann et al., 2013). Seven of the S/T-Q phosphorylation sites (9–15 S/T-Q sites) are required for interaction between RIF1 and 53BP1, whereas PTIP binds directly to the first eight S/T-Q sites in the N-terminal region. Loss of either RIF1 or PTIP partially alleviates HR defects in BRCA1-deficient cells, suggesting that 53BP1 phosphorylation influences resection in a BRCA1-dependent manner. However, the functional significance of 53BP1 phosphorylation in S/G_2 phase, especially in the context of switching from NHEJ to HR, remains unexplored.

In this study, we found that 53BP1 can be phosphorylated in S/G_2 phase, and that RIF1 is transiently recruited to DSB sites. This finding supports the notion that establishment of the 53BP1 barrier allows NHEJ to be the first choice pathway even in S/G_2 phase. Next, we dissected the role of BRCA1 and CtIP/MRE11 nuclease in resection, showing that impaired resection by CtIP depletion or MRE11 endonuclease inhibition sustains RIF1 at DSB sites due to ongoing ATM signaling. In contrast, depletion of BRCA1 attenuates 53BP1 dephosphorylation, resulting in RIF1 accumulation. Furthermore, a small interfering RNA (siRNA) screen of protein phosphatases identified PP4C/PP4R2 as a major phosphatase responsible for dephosphorylating 53BP1 and releasing RIF1. Finally, we demonstrate that BRCA1 and PP4C promote resection by removing RIF1 from DSBs, leading to 53BP1 repositioning, EXO1 recruitment, and extensive resection in HR. Collectively, our findings show that RIF1 retention in BRCA1-depleted cells is the cause of the resection defect rather than the consequence of it. Thus, we have uncovered a key role for BRCA1 in directing DSB repair pathway from NHEJ to HR by coordinating 53BP1 phosphorylation status in S/G_2 phase.

RESULTS

53BP1 Is Phosphorylated by ATM in S/G_2 Phase, Followed by Transient RIF1 Recruitment

ATM-dependent 53BP1 phosphorylation recruits RIF1, forming a barrier against resection in G_1 phase (Escribano-Díaz et al., 2013). Therefore, it was expected that 53BP1 phosphorylation would be suppressed in S/G_2 phase, where HR functions to repair DSBs. However, because ATM contributes to checkpoint activation throughout the cell cycle and is required for resection in HR, ATM activation occurs even in S/G_2 phase (Jeggo and Löbrich, 2006; Shibata et al., 2011). To resolve this paradoxical observation, we examined 53BP1 phosphorylation and RIF1 recruitment to DSBs in G_2 phase by quantifying 53BP1-pT543 (a phosphorylation site required for RIF1 recruitment), RIF1, RPA (a resection marker), and γH2AX/53BP1 (a DSB marker) foci in irradiated G_2 cells (Figures 1A–1C and S1). G_2 cells were identified by CENPF staining (Shibata et al., 2011, 2014). The results revealed a transient increase in the number of 53BP1-pT543 and RIF1 foci 5–30 min in G_2 after ionizing radiation (IR). However, the number of 53BP1-pT543 foci then decreased for up to 2 hr post-IR. RIF1 foci persisted slightly longer than 53BP1-pT543 foci, but most had disappeared by 2 hr, a time when γH2AX/53BP1 foci remain. Importantly, loss of 53BP1-pT543 and RIF1 foci was associated with RPA foci formation, indicating the onset of resection (Shibata et al., 2011). To determine whether loss of 53BP1-pT543 and RIF1 was specific to G_2 cells, we examined irradiated G_1 cells (Figure 1D). The disappearance of 53BP1-pT543 and RIF1 foci in cells in G_1 occurred at later times concomitant with the decrease in γH2AX/53BP1 foci. These data suggest that ATM phosphorylates 53BP1 in both G_1 and G_2 phases; however, 53BP1 phosphorylation and RIF1 recruitment rapidly decrease in G_2, whereas they are sustained in G_1 phase (Figure 1E). To extend these findings to S phase, we treated cells with camptothecin (CPT), which causes replication damage. After CPT treatment, RPA-pS4/8 (a marker of resection) increased with time in S-phase cells (Figure 1F). Importantly, the transient increase in 53BP1-pT543 and RIF1 recruitment was observed immediately after CPT release (Figures 1F and 1G). Together, these results demonstrate that 53BP1 can be phosphorylated by ATM in S/G_2 phase, followed by RIF1 recruitment, which occurs transiently. Subsequently, loss of 53BP1-pT543 and RIF1 foci occurs concomitantly with the progression of resection in HR.

Impaired Initiation of Resection by CtIP Depletion or MRE11 Endonuclease Inhibition Sustains RIF1 at DSB Sites

DNA-end resection is orchestrated by several nucleases (Symington and Gautier, 2011). MRE11 endonuclease activity initiates resection and the exonuclease activities of MRE11, EXD2, and EXO1/BLM digest DNA for extensive resection (Broderick et al., 2016; Garcia et al., 2011; Shibata et al., 2014; Zhu et al., 2008). To ask whether the DNA nuclease activities are involved in RIF1 release, we examined RIF1 foci in G_2 following treatment with MRE11 inhibitors. We confirmed that depletion of BRCA1 or CtIP impaired RIF1 release in irradiated G_2 cells but not in G_1 cells (Figure 2A). At 4 hr after IR, no RIF1 and 53BP1-pT543 foci were observed in control cells, whereas RIF1 and 53BP1-pT543 foci were sustained in cells treated with a specific MRE11 endonuclease inhibitor (Figure 2B). Inhibition of MRE11 exonuclease activity had no effect on RIF1, although there is a marginal increase in 53BP1-pT543 foci (Figures 2B and S2). Depletion of EXO1/BLM causes RIF1 and 53BP1-pT543 foci to be partially sustained (Figures 2B and S2). However, combined EXO1/BLM depletion and MRE11 exonuclease inhibition, which fully inhibits resection, reduced RIF1 release to a degree similar to that of CtIP depletion (Figures 2B–2D and S2) (Shibata et al., 2014). Thus, RIF1 release requires resection. Next, to address whether the resection defect caused by CtIP/MRE11/EXO1 inhibition/depletion or BRCA1 depletion causes RIF1 retention or is a consequence of RIF1 presence, we examined whether RIF1 depletion alleviates the resection defect in these cells. Importantly, depletion of RIF1 rescued resection in BRCA1 siRNA cells but not in CtIP siRNA,

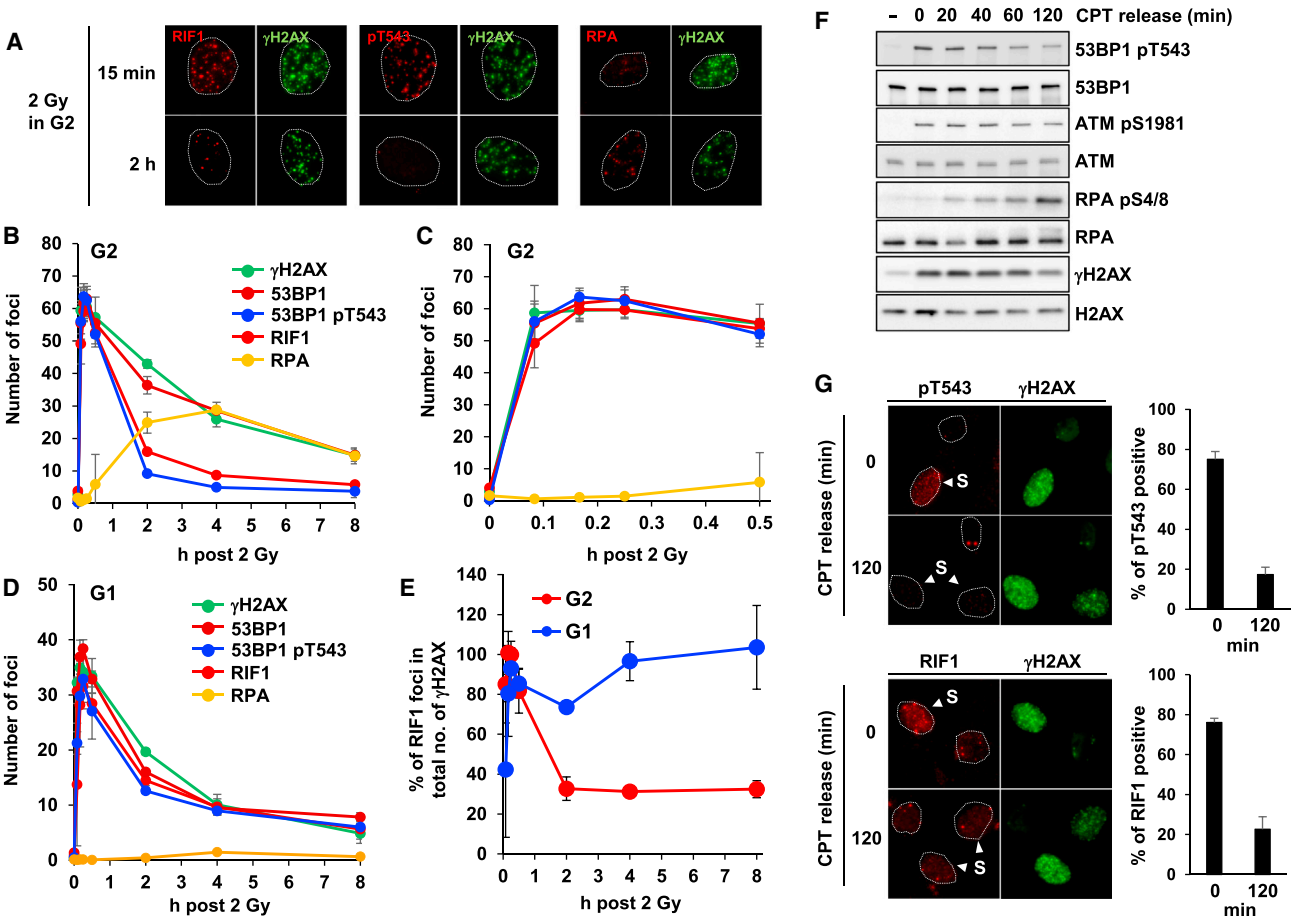

Figure 1. 53BP1 Is Phosphorylated by ATM in S/G_2 Phase, Followed by Transient RIF1 Recruitment

(A–C) Loss of 53BP1-pT543 and RIF1 foci is associated with progression of DNA-end resection in irradiated cells in G_2. 1BR (WT) hTERT cells were fixed and stained with γH2AX, 53BP1, 53BP1-pT543, RIF1, or RPA at the indicated time points after irradiation with 2 Gy. Aphidicolin (APH) was added 30 min prior to IR, to prevent the progression of irradiated cells from S to G_2 (Shibata et al., 2011). G_2 cells were identified by CENPF staining (full images and ATM-dependent 53BP1-pT543 and RIF1 foci formation are shown in Figure S1). Specificity of the 53BP1-pT543 antibody was verified in 53BP1 T543A mutant cells (Figure S1). Earlier time points in the experiment of (B) are enlarged in (C).

(D) γH2AX, 53BP1, 53BP1-pT543, RIF1, or RPA foci were analyzed in 1BR (WT) hTERT G_1 cells.

(E) The percentage of RIF1/γH2AX foci in cells in G_2 and G_1 is shown.

(F) Loss of 53BP1-pT543 is associated with progression of resection after treatment with CPT. 53BP1-pT543, ATM-pS1981, RPA-pS4/8, and γH2AX were examined in A549 cells following treatment with 2 μM CPT for 30 min.

(G) Transient 53BP1-pT543 and RIF1 recruitment in γH2AX-positive 1BR hTERT cells was detected by immunofluorescence staining after treatment with CPT. The percentage of 53BP1-pT543- or RIF1-positive cells as a percentage of γH2AX-positive cells is shown in the right panel.

Values in (B)–(E) and (G) are means ± SEM from three independent experiments. In (A) and (F), a similar result is obtained from more than two independent experiments.

MRE11 endonuclease-inhibited, and EXO1/BLM siRNA plus MRE11 exonuclease inhibitor-treated cells (Figure 2C). These data demonstrate that CtIP and the nucleases have direct roles in promoting resection irrespective of whether RIF1 is present or absent as expected, whereas BRCA1 has a distinct and unique role in promoting release of RIF1, which impacts downstream of the initiation of resection.

BRCA1 Promotes Dephosphorylation of 53BP1 and Release of RIF1 from DSB Sites

Because 53BP1-pT543 foci in G_2 rapidly disappear at 30–60 min post-IR (Figures 1A–1C), we speculated that 53BP1 phosphorylation may be sustained by ongoing ATM signaling from DSB ends with rapid turnover. To test this, we treated cells with an ATM inhibitor (ATMi) at the peak of 53BP1-pT543 foci formation, i.e., 15 min post-IR (hereafter called ATMi post-IR), enabling the initiation of resection to take place but not ongoing ATM signaling (Figure 3A). Strikingly, 53BP1-pT543 was drastically reduced by ATMi post-IR (Figure 3B). To examine whether ongoing ATM signaling influences 53BP1-pT543 and RIF1 maintenance at DSB sites, 53BP1-pT543 and RIF1 foci were scored following ATMi treatment post-IR (Figures 3C and S3A). Inhibition of ATM signaling rapidly diminished 53BP1-pT543 and RIF1 foci, although γH2AX foci were not significantly affected,

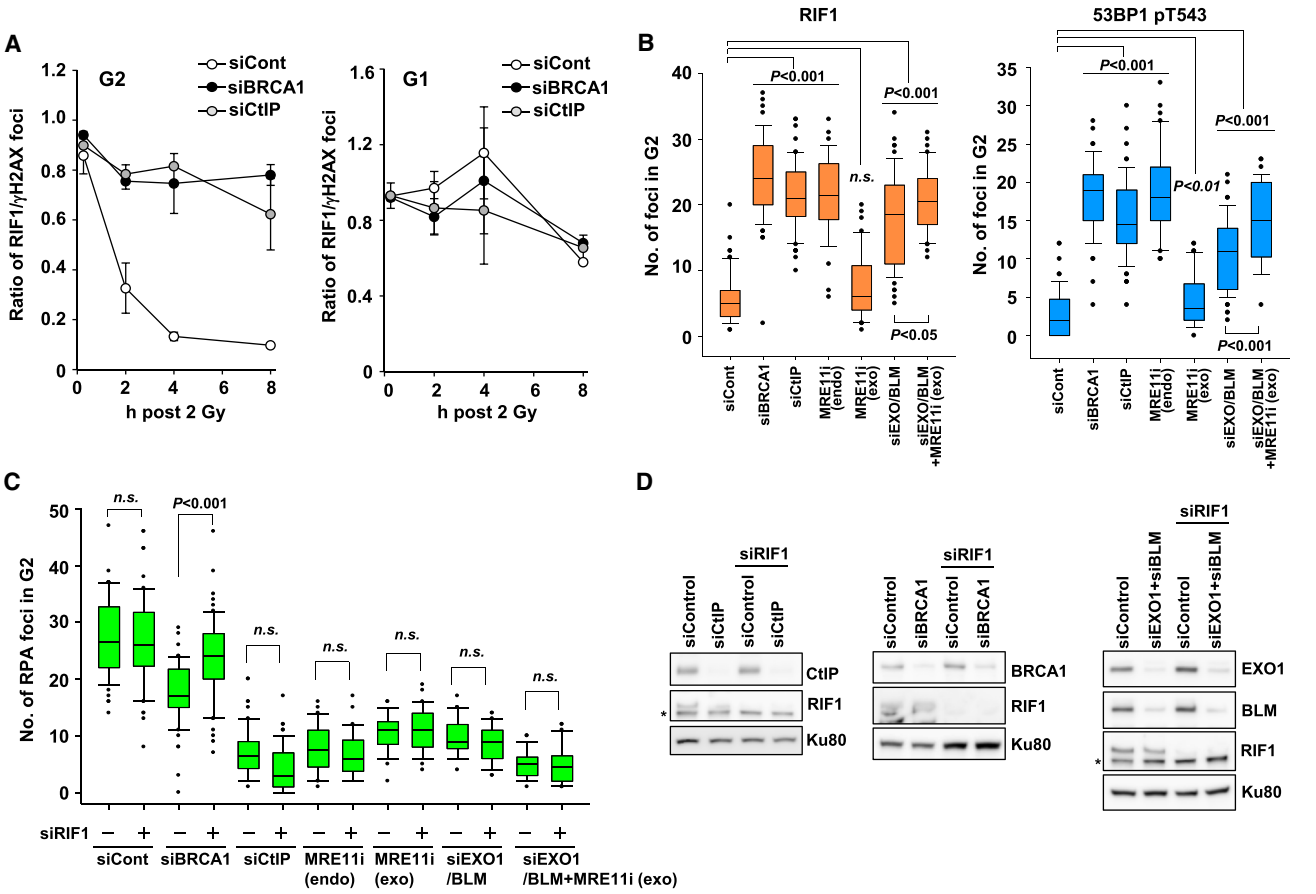

Figure 2. Impaired Resection by CtIP Depletion or MRE11 Endonuclease Inhibition Sustains RIF1 at DSB Sites

(A) Depletion of BRCA1 or CtIP attenuates RIF1 release in irradiated G_2, but not in G_1. The ratio of RIF1/γH2AX foci at each time point was examined in A549 cells following depletion of BRCA1 or CtIP.

(B) Impaired resection by CtIP depletion or MRE11 endonuclease inhibition sustains RIF1 and 53BP1-pT543 foci at DSB sites. RIF1 or 53BP1-pT543 foci in A549 cells following depletion of BRCA1 or CtIP, or treatment with MRE11 inhibitors and/or EXO1/BLM depletion was examined in G_2 cells 4 hr after 2 Gy. PFM01 and PFM39 were used as MRE11 endonuclease or exonuclease inhibitors, respectively. Representative images are shown in Figure S2.

(C) RIF1 depletion rescued the resection defect observed following BRCA1 depletion but not following CtIP depletion, inhibition of MRE11 endonuclease activity, or EXO1/BLM depletion combined with inhibition of MRE11 exonuclease activity. RPA foci in A549 G_2 cells were scored at 2 hr after 1 Gy.

(D) Knockdown efficiency in A549 cells is shown. Asterisk indicates non-specific bands.

Values in (A) are means ± SEM from three independent experiments. In (B) and (C), a similar result is obtained from more than two independent experiments. The p values were derived from Student's two-tailed t test or Mann-Whitney U test.

likely due to redundant phosphorylation by DNA-PKcs (Stiff et al., 2004).

Depletion/inhibition of CtIP/MRE11 endonuclease activity, which precludes the initiation of resection, causes sustained RIF1 at DSB sites (Figures 2B and 2C). However, depletion of RIF1 did not rescue resection. By contrast, depletion of RIF1 did allow resection in BRCA1-depleted cells (Figure 2C) (Escribano-Díaz et al., 2013). We therefore hypothesized that BRCA1 functions to promote 53BP1 dephosphorylation to remove the RIF1 barrier to resection, rather than having a direct role in resection itself. To examine whether BRCA1 influences 53BP1-pT543 in the absence of ongoing ATM signaling, we treated BRCA1-depleted cells with ATMi post-IR, and monitored the stability of 53BP1-pT543 and RIF1 foci in irradiated G_2 cells. Strikingly, after ATMi post-IR, 53BP1-pT543 and RIF1 foci were sustained in BRCA1-depleted cells, whereas they rapidly disappeared in control, CtIP siRNA, MRE11 endo-inhibition, or EXO1/BLM siRNA plus MRE11 exo-inhibition cells (Figures 3D–3F and S3B). This result shows that the maintained 53BP1-pT543 (and hence RIF1 foci) observed in CtIP-depleted cells arises as a consequence of ongoing ATM signaling. We propose that this occurs at unresected DNA ends in CtIP-depleted cells (Shiotani and Zou, 2009). Next, we considered that the phosphorylation of the CtIP S327 residue might be required for the function of BRCA1 in RIF1 release. However, RIF1 foci rapidly disappeared in cells expressing a CtIP-siRNA-resistant CtIP S327A mutant plus ATMi post-IR, suggesting that the phosphorylation of S327 in CtIP is dispensable for RIF1 retention (Figure S3C). Furthermore, depletion of RIF1 did not significantly affect 53BP1-pT543 foci, even though an interaction between RIF1

and the protein phosphatase PP1 has been reported (Figure 3F) (Davé et al., 2014). To confirm the persistence of 53BP1-pT543 foci in BRCA1-depleted cells, we developed a fluorescence-activated cell sorting (FACS) assay to monitor 53BP1-pT543 in irradiated S/G_2 cells. 53BP1-pT543 was lost in control S/G_2 cells but sustained in S/G_2 BRCA1-depleted cells (Figures 3G and S3D).

Together, our data demonstrate that BRCA1 promotes 53BP1 dephosphorylation, resulting in RIF1 release. Conversely, depletion/inhibition of CtIP/MRE11 endonuclease activity results in sustained 53BP1 phosphorylation and RIF1 due to ongoing ATM signaling (i.e., it is inhibited by ATMi post-IR). We propose that ATM signaling is ongoing at un-resected DSB ends due to the lack of initiation of resection.

PP4C Dephosphorylates 53BP1, Promoting RIF1 Release from DSB Sites

Next, to identify the protein phosphatase involved in dephosphorylation of 53BP1 and subsequent RIF1 release, we performed an siRNA screen by monitoring RIF1 foci in cells in G_2 (Figures 4A and S4A). The screen revealed that PP4C depletion causes substantial inhibition of RIF1 release, suggesting that PP4C is a major phosphatase for 53BP1 in the context of RIF1 release (Figures 4B, 4C, and S4B). Similar results were obtained using a different siRNA oligo for PP4C (Figures S4C–S4E). Depletion of PP1CB also resulted in reduced RIF1 release; however, 53BP1-pT543 levels were only modestly increased compared to PP4C-depleted cells (Figures 4B, 4C, and S4B–S4E). Depletion of PP3CB or PP3CC also showed delayed RIF1 release in the first screen. However, this was not reproduced using other siRNA oligos (Figure S4F). Attenuation of 53BP1 dephosphorylation in PP4C-depleted cells was confirmed by FACS analysis (Figure 4D). To confirm the requirement of PP4C phosphatase activity for RIF1 release, we exogenously expressed PP4C in U2OS cells (Figure 4E). Expression of wild-type (WT) PP4C, but not the phosphatase-inactive R86A mutant (Nakada et al., 2008), impaired transient RIF1 foci formation in cells in G_2. To exclude any potential off-target effects of the siRNA, we reintroduced siRNA-resistant forms of PP4C into PP4C-depleted cells (Figure 4F). Re-expression of wild-type PP4C restored RIF1 release in PP4C-siRNA cells, but the PP4C phosphatase-inactive mutant did not, demonstrating that PP4C phosphatase activity is required for RIF1 release. Furthermore, to identify which regulatory subunit of PP4 is required for 53BP1-pT543 dephosphorylation, we analyzed RIF1 and 53BP1-pT543 foci in G_2 cells following siRNA targeting of all PP4 regulatory subunits (Figure S4G). This analysis revealed that PP4R2 is required for 53BP1-pT543 dephosphorylation (Figure 4G). RIF1 also failed to be released in PP4R2-depleted cells. Next, we performed co-immunoprecipitation between BRCA1 and PP4C but could not detect any interaction with or without DNA damage (Figure S5A). To gain insight into the spatial interaction between BRCA1 and PP4C in G_2, we performed an in situ proximity ligation assay (PLA) and observed an increase in the BRCA1-PP4C PLA signal after IR (Söderberg et al., 2006) (Figures S5B–S5E: control experiments are shown in Figures S5B and S5C). Next, we utilized the PLA assay to examine whether 53BP1-pT543 and PP4C interact in G_2. Significantly, the PLA signal from 53BP1-pT543 and PP4C was increased at 10–20 min after IR, which is consistent with the timing of disappearance of 53BP1-pT543 and RIF1 foci in G_2 (Figures 1A–1C, S5F, and S5G). However, the spatial proximity was not significantly affected by depletion of BRCA1, suggesting that BRCA1 is not directly mediating the interaction between 53BP1-pT543 and PP4C (Figure S5H).

Collectively, our observations suggest that that PP4C activity is required for dephosphorylation of 53BP1-pT543 and RIF1 release in G_2 phase and that this is promoted in the presence of BRCA1.

53BP1 Phosphorylation Is Required to Maintain RIF1 in the BRCA1-PP4C Pathway

RIF1 recruitment on chromatin is dependent on the phosphorylation of the N-terminal 53BP1 7S/TQ sites (Callen et al., 2013; Chapman et al., 2013). To verify the requirement for phosphorylation of 53BP1 in RIF1 retention in BRCA1- or PP4C-depleted cells, we examined RIF1 foci in G_2 cells expressing siRNA-resistant 53BP1 phosphor mutants following 53BP1 siRNA (Figures 5A–5C). In control G_2 cells, RIF1 foci were not observed at 4 hr post-IR. As expected, no RIF1 foci were observed at 4 hr post-IR in cells expressing the 7A mutant following BRCA1 or PP4C depletion consistent with the previous conclusion that these seven phosphorylation sites are required for RIF1 recruitment (Figure 5C). Throughout this study, we have used a 53BP1-pT543 antibody to assess the phosphorylation status within the 7S/TQ sites. To assess whether phosphorylation of T543 affects RIF1 retention in BRCA1- or PP4C-depleted cells, we examined RIF1 foci in cells expressing a T543A mutant (6 S/TQ sites are wild type) and a 6A mutant (in which only T543 is wild type). Unlike the 7A mutant, the T543A mutant (six S/TQ sites are wild type) formed and retained RIF1 foci at 4 hr post-IR in BRCA1- or PP4C-depleted cells (Figure 5C). This result suggests that phosphorylation of the six S/TQ sites (i.e., excluding T543) is sufficient to retain RIF1 on chromatin. In contrast, surprisingly, the 6A mutant (T543 wild type) also retained RIF1 in BRCA1- or PP4C-depleted cells (Figure 5C), suggesting that phosphorylation of T543 alone is sufficient to sustain RIF1. Taken together, these data support the notion that phosphorylation of T543 alone can tether RIF1 on chromatin but in its absence the other sites can suffice, i.e., phosphorylation of the seven S/TQ sites redundantly contributes to RIF1 retention. Thus, although T543 phosphorylation may not be essential for RIF1 recruitment, loss of its phosphorylation (i.e., dephosphorylation) is essential for RIF1 loss. Thus, our 53BP1-pT543 antibody is a valid readout to monitor a phosphorylation event required for RIF1 loss following its initial recruitment in G_2 cells.

RIF1 Release Relieves the 53BP1 Barrier to Recruit EXO1 at Damage Sites

Recent studies revealed that BRCA1-dependent 53BP1 repositioning occurs prior to resection because a defect in 53BP1 repositioning in BRCA1- or POH1-depleted cells attenuates resection (Chapman et al., 2012a; Kakarougkas et al., 2013). Similar to the situation in BRCA1-depleted cells, we found that 53BP1 foci enlargement was impaired by depletion of PP4C (Figures 6A, 6B, and S6A). Moreover, depletion of RIF1 restored 53BP1 foci

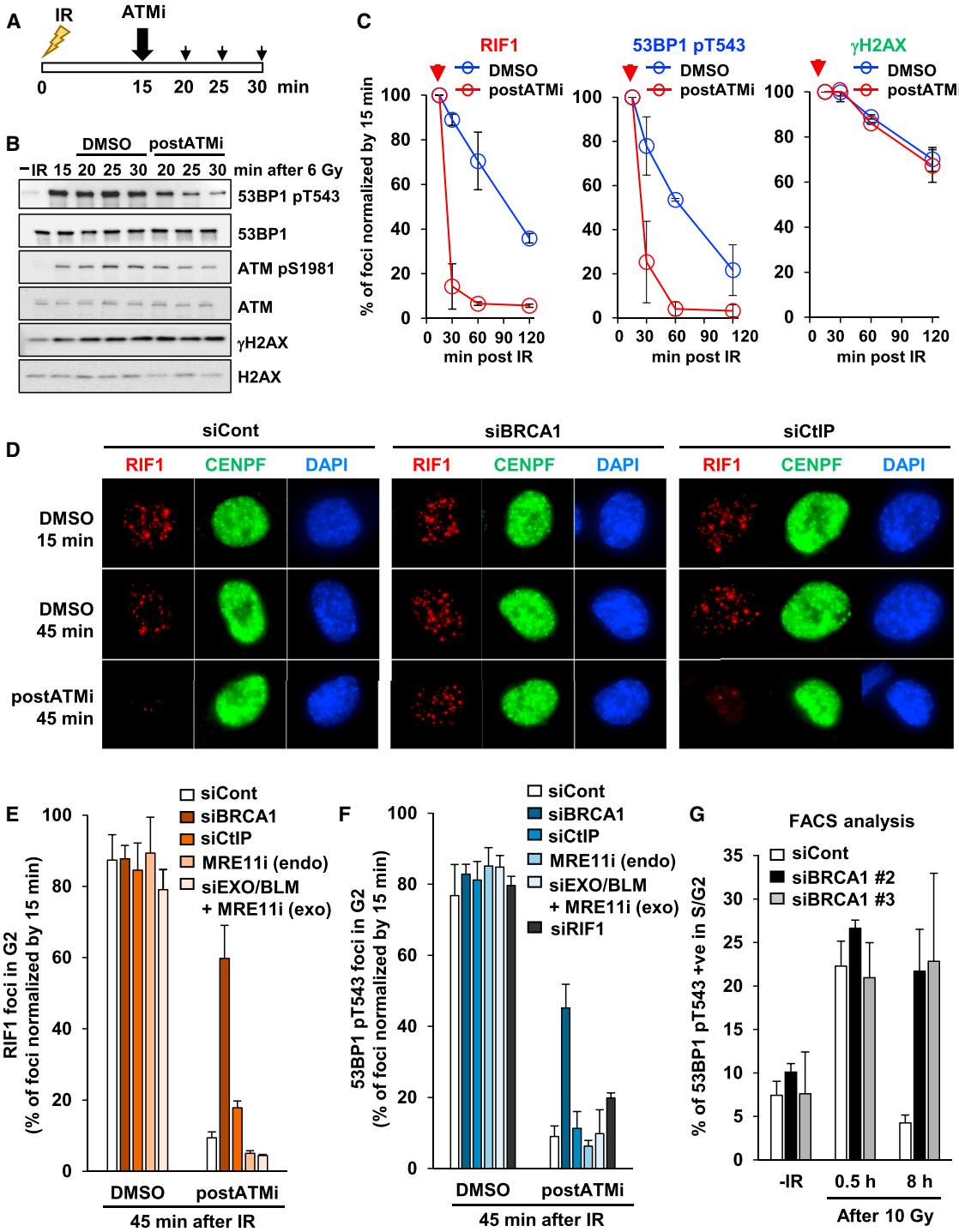

Figure 3. BRCA1 Promotes Dephosphorylation of 53BP1, Resulting in Release of RIF1 from DSB Sites

(A and B) Phosphorylation of 53BP1 at T543 rapidly disappeared when ATM signaling was inhibited. ATMi, which shuts down ATM activity within a few minutes (Lee et al., 2012), was added 15 min after IR to prevent ongoing ATM signaling after the initial recruitment of RIF1, but not inhibit the initiation of resection. The experimental scheme is shown in (A). Turnover of phosphorylated proteins was examined in A549 cells with or without post-ATMi after irradiation with 6 Gy.

(C) 53BP1-pT543 and RIF1 foci in G_2 cells are more persistent under conditions of continuous ATM signaling. 53BP1-pT543 or RIF1 foci at the indicated time points were normalized to the number of γH2AX foci 15 min after irradiation with 2 Gy. 1BR (WT) hTERT cells were irradiated with 2 Gy and treated with ATMi 15 min post-IR. The numbers of 53BP1-pT543, RIF1, and γH2AX foci are shown in Figure S3A.

(D) Representative images of RIF1 foci in siControl, siBRCA1, or siCtIP cells ± ATMi are shown. ATMi was added 15 min after 2 Gy.

(legend continued on next page)

enlargement in BRCA1- and PP4C-depleted cells (Figures 6A, 6B, and S6A–S6D). Depletion of RIF1 accelerated the speed of resection, indicating that RIF1 may function to protect DNA ends early in DSB repair, i.e., during NHEJ (Feng et al., 2013) (Figure 6C). We therefore examined whether the role of RIF1 foci formation at early times after IR might be to prevent 53BP1 repositioning to generate pro-NHEJ environment. To address this question, we examined 53BP1 foci size in RIF1-depleted G_2 cells at 30 min after IR, a time at which control cells do not show 53BP1 foci enlargement and resection is not progressed (Kakarougkas et al., 2013). Importantly, we observed that RIF1 depletion caused substantial enlargement of 53BP1 foci even at this early time (Figures 6D and S6E). Next, we speculated that 53BP1 repositioning following RIF1 release may allow EXO1 recruitment for the second step of resection. To examine the kinetics of EXO1 recruitment at DNA damage sites, we measured the intensity of recruited GFP-EXO1 at UV laser tracks (Figures 6E and S7). Importantly, EXO1 recruitment was significantly reduced by depletion of BRCA1 or PP4C and the reduction was rescued by 53BP1 depletion (Figure 6E). These data suggest that 53BP1 repositioning is restricted or precluded by the presence of RIF1, but following the recruitment of BRCA1 with time, PP4C-dependent 53BP1 dephosphorylation releases RIF1, causing 53BP1 repositioning to facilitate the EXO1-dependent second step resection. This consolidates the notion that the initial recruitment of RIF1 delays resection, which, we propose, allows the possibility for NHEJ to take place.

PP4C Promotes DNA-End Resection and HR in the 53BP1-BRCA1 Axis

To address whether PP4C-dependent RIF1 release contributes to resection, we analyzed RPA/RAD51 foci formation after IR. Depletion of PP4C reduced RPA/RAD51 foci formation in irradiated G_2 cells (Figure 7A). Importantly, these defects were restored by RIF1 depletion (Figure 7A). Furthermore, to examine whether resection is impacted by 53BP1 phosphorylation status, we monitored RPA foci formation in 53BP1 phosphor mutants with or without BRCA1 or PP4C siRNA. Consistent with the results assessing RIF1 release (Figure 5), the 7A mutant restored resection in BRCA1- or PP4C-depleted cells, whereas neither the 6A nor the T543A mutant alleviated the resection defect in BRCA1- or PP4C-depleted cells (Figure 7B). To assess HR activity in PP4C-depleted cells, we exploited an HR reporter assay using cells with chromosomally integrated I-*Sce*I-inducible DSBs and observed a decrease in HR in PP4C-depeleted cells (Figure 7C). This defect was restored by depletion of 53BP1 or RIF1. Together, these results suggest that PP4C promotes DNA-end resection and HR in the 53BP1/RIF1-BRCA1 axis. Finally, clonogenic survival analysis showed that PP4C depletion resulted in hypersensitivity to CPT, which could be reversed by 53BP1 depletion (Figure 7D). Together, these results suggest that transient 53BP1 phosphorylation and RIF1 recruitment in S/G_2 phase play a role in maintaining and regulating the 53BP1 barrier, which inhibits excessive resection (Figure 7E).

DISCUSSION

Previous studies showed that RIF1 is recruited to DSBs in G_1 phase to restrict resection and promote NHEJ (Escribano-Díaz et al., 2013). Here, we show that RIF1 is also recruited to DSBs in S/G_2 phase but only transiently, with its loss being essential for the progression of HR. Thus, whereas in G_1 phase, RIF1 foci loss correlates with DSB repair assessed by γH2AX foci, in G_2 phase, RIF1 foci are lost earlier than γH2AX foci. Additionally, we show that BRCA1 is dispensable for the recruitment of RIF1 in G_2 cells but is required for its timely release. Timely release of RIF1 can, in a 6A mutant, be regulated by phosphorylation/dephosphorylation of 53BP1-T543, allowing us to use phosphor-specific antibodies for this site to assess the process. Resection during HR has been separated into a CtIP/MRE11 endonuclease-dependent initiation step and an elongation step involving the exonucleases, MRE11, EXO1, and EXD2 (Broderick et al., 2016; Shibata et al., 2014). Failure to initiate resection does not cause a repair defect because DSBs can undergo repair by NHEJ, whereas failure to elongate resection precludes the use of NHEJ and HR, conferring a repair defect (Kakarougkas et al., 2013; Shibata et al., 2014). Depletion of BRCA1 causes HR defects due to a block at the stage of extending resection in G_2 (Kakarougkas et al., 2013). Although a role for BRCA1 in promoting resection is well accepted, its precise function is unclear. Here, we show that BRCA1 promotes RIF1 release from 53BP1 via a process involving PP4C. Although loss of RIF1 does not rescue resection in nuclease-defective cells, resection in siBRCA1 cells is rescued by RIF1 depletion, demonstrating that BRCA1 is dispensable for the nuclease activities but is required to relieve the RIF1 block, which is consistent with the accepted finding that BRCA1 relieves the block to resection posed by 53BP1, the factor required for RIF1 recruitment.

The maintenance of RIF1 foci requires ongoing ATM signaling (i.e., from 5 to 15 min post-IR). The number of RIF1/53BP1-pT543 foci at these time points in G_2 is similar to γH2AX foci. Thus, we propose a working model that ATM activation at all the DSBs leads to N-terminal 53BP1 phosphorylation and RIF1 recruitment. In G_2 cells, ~70% DSBs are rapidly repaired by

(E) Depletion of BRCA1 attenuates RIF1 release following inhibition of ongoing ATM signaling. RIF1 foci were examined in 1BR (WT) hTERT cells treated with siControl, siBRCA1, siCtIP, MRE11 endonuclease inhibitor or siEXO1/BLM plus MRE11 exonuclease inhibitor. Cells were fixed at 30 min with or without ATMi 15 min after 2 Gy. PFM01 and PFM39 were used as MRE11 endonuclease and exonuclease inhibitor. The percentage of foci at 45 min with or without ATMi is normalized by foci at 15 min.

(F) 53BP1-pT543 foci were examined in 1BR (WT) hTERT cells. ATMi was added 15 min after 2 Gy.

(G) Depletion of BRCA1 sustains IR-induced 53BP1-pT543 in S/G_2. IR-induced 53BP1-pT543 in S/G_2 cells was analyzed by FACS. A549 cells transfected with Control or BRCA1 siRNA were fixed 0.5 and 8 hr after irradiation with 10 Gy. Cells were labeled with Alexa Fluor 488 and propidium iodide (PI). FACS plots are shown in Figure S3D.

Values in (C) and (E)–(G) are means ± SEM from three independent experiments. In (B) and (D), a similar result is obtained with more than two independent experiments.

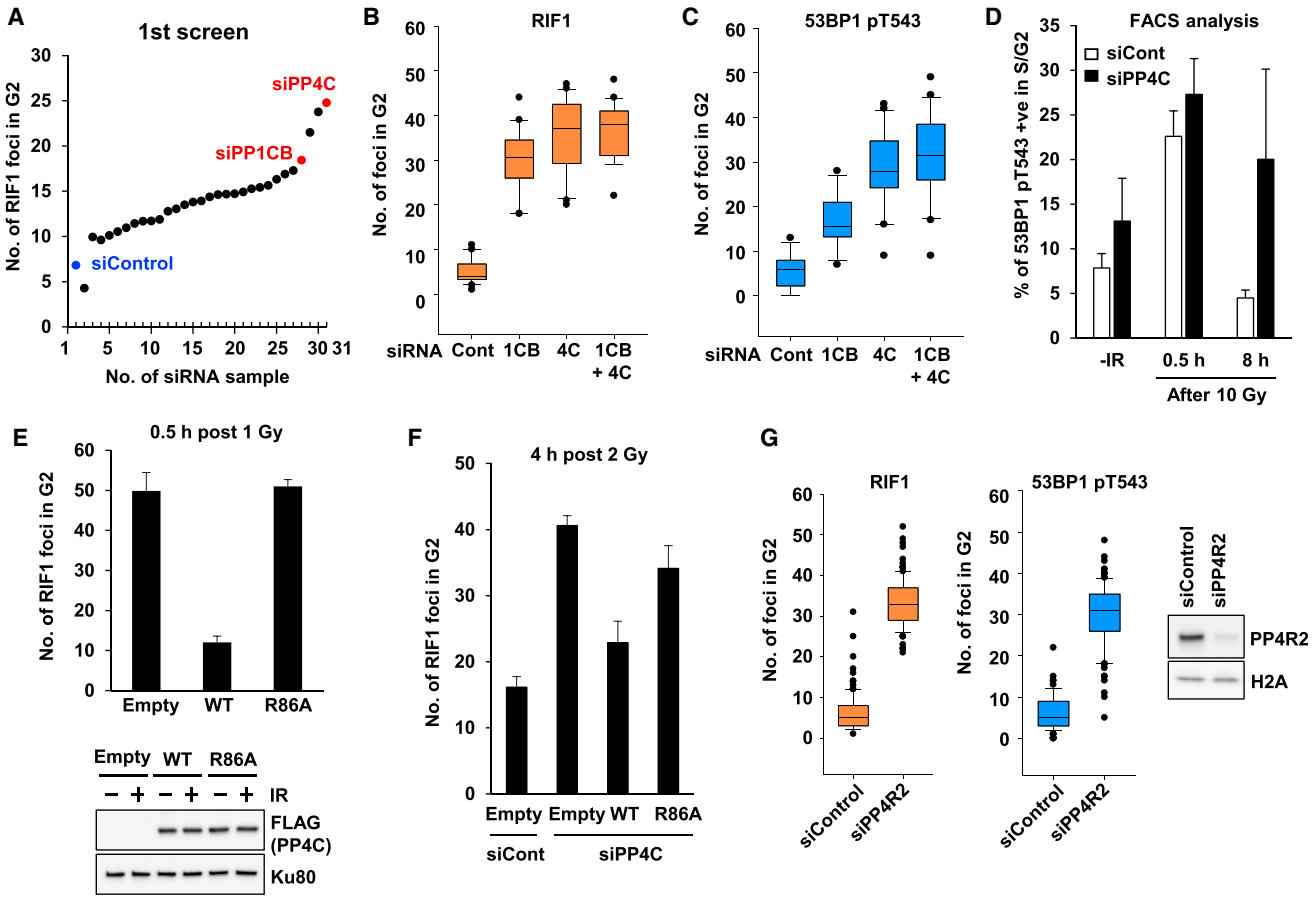

Figure 4. PP4C Dephosphorylates 53BP1, Promoting RIF1 Release from DSB Sites

(A) Screen of protein phosphatases against 53BP1-pT543 was performed using a phosphatase siRNA library in A549 cells. The list of genes is shown in Figure S4A. RIF1 foci in G_2 were enumerated 2 hr after irradiation with 2 Gy.

(B) RIF1 foci in G_2 were scored in PP1CB- and/or PP4C-depleted A549 cells at 4 hr after irradiation with 2 Gy. Degree of knockdown is shown in Figure S4B. A similar result was obtained using a second set of siRNAs (Figures S4C–S4E).

(C) 53BP1-pT543 foci in G2 were scored in PP1CB- and/or PP4C-depleted A549 cells at 4 hr after irradiation with 2 Gy.

(D) 53BP1-pT543 is sustained by depletion of PP4C. A549 cells were collected at 30 min and 8 hr after irradiation with 10 Gy with or without siPP4C. 53BP1-pT543 levels in cells in S/G_2 phase were measured by FACS.

(E) Expression of exogenous PP4C promotes RIF1 release. U2OS cells were transfected with FLAG-empty, FLAG-wild-type PP4C (WT) or FLAG-catalytically inactive PP4C mutant (R86A) expression vectors. Flag-PP4C expression levels are shown in the right panel.

(F) siRNA-resistant PP4C expression restores the phenotype of control cells. U2OS cells transfected with PP4C siRNA were transfected with FLAG-empty, FLAG-PP4C WT, or FLAG-PP4C R86A mutant expression vectors.

(G) Depletion of PP4R2 sustained RIF1 and 53BP1-pT543 foci in G_2. PP4R2 siRNA-treated A549 cells were fixed at 4 hr post 2 Gy. Knockdown efficiency is shown in the right panel.

Values in (D)–(F) are means ± SEM from three independent experiments. In (B), (C), and (G), a similar result is obtained from more than two independent experiments.

~1–2 hr post-IR. Subsequent BRCA1 recruitment, which takes longer than RIF1 foci, then promotes PP4C-dependent dephosphorylation of 53BP1, ultimately leading to RIF1 release at DSBs undergoing repair by HR. As resection progresses, it is known that the active kinase shifts from ATM to ATR, and to date, the significance of this switch has not been appreciated (Shiotani and Zou, 2009). The decrease in RIF1 and 53BP1-pT543 foci following ATM inhibition post-IR strongly suggests that ATR does not phosphorylate 53BP1 at the sites required for RIF1 recruitment. Importantly, although attenuation of ATM enhances RIF1 loss, the process additionally requires BRCA1 and the dephosphorylation activity of PP4C. Thus, we propose a competitive feedback loop with ATM phosphorylation competing with PP4C dephosphorylation. As resection progresses, ATM activity is diminished until PP4C activity out-competes ATM phosphorylation activity at the 53BP1 sites and RIF1 is finally lost.

RIF1 was previously identified as another antagonist of BRCA1 and previous studies have suggested a role in DNA-end protection (Callen et al., 2013; Chapman et al., 2013; Escribano-Díaz

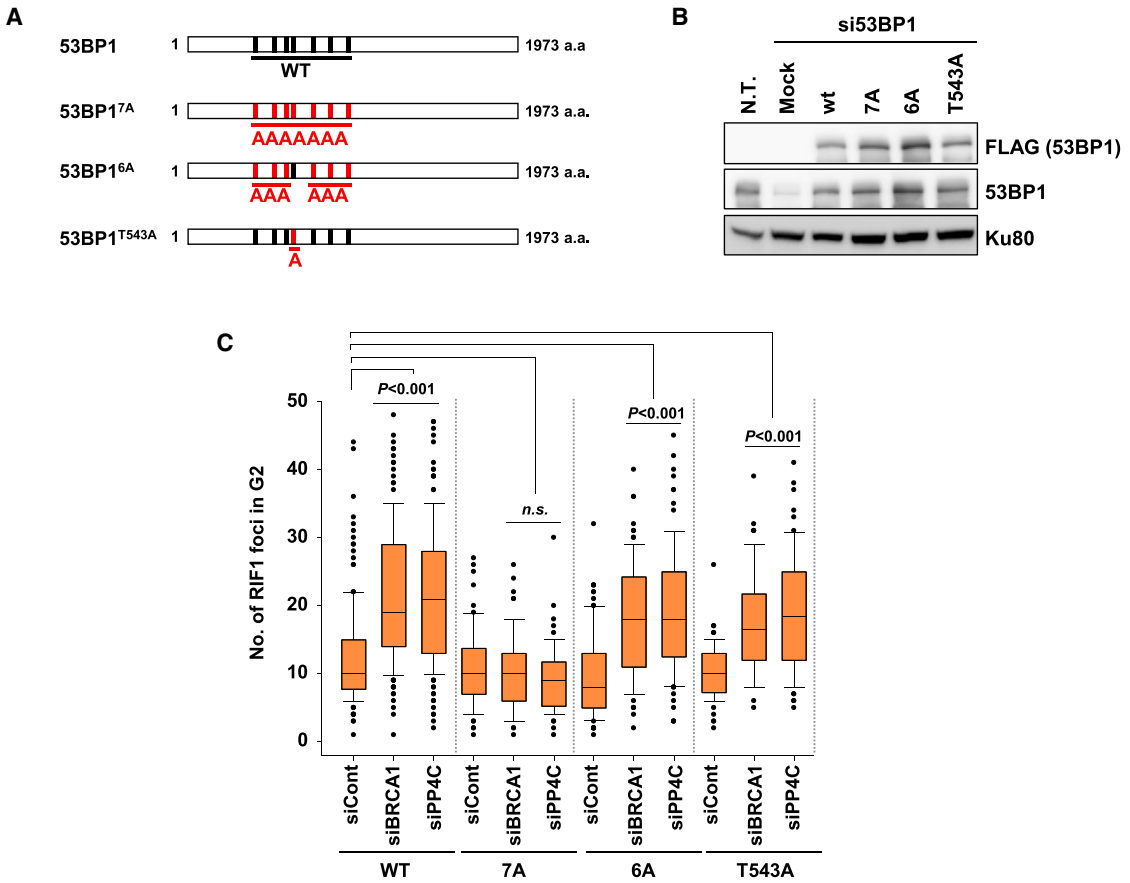

Figure 5. Analysis of RIF1 Foci in 53BP1 Phosphor Mutants

(A) Schematic representation of siRNA-resistant 53BP1 phosphor mutants. 7A mutant: T302A, S452A, S523A, T543A, S625A, S784A, and S892A. 6A mutant: T302A, S452A, S523A, S625A, S784A, and S892A.

(B) siRNA-resistant FLAG-53BP1 WT or phosphor mutants were expressed efficiently in A549 cells.

(C) Analysis of RIF1 foci formation in 53BP1 phosphor mutants. RIF1 foci at 4 hr post 2 Gy was analyzed in A549 cells expressing siRNA-resistant FLAG-53BP1 WT, 7A, 6A, or T543A following 53BP1 siRNA with or without Control, BRCA1, or PP4C siRNA.

In (B) and (C), a similar result is obtained with more than two independent experiments. The p values were derived from Student's two-tailed t test or Mann-Whitney U test.

et al., 2013; Zimmermann et al., 2013). Similar to previous findings, we showed that resection is mildly increased at early time points in RIF1-depleted cells (Feng et al., 2013). Interestingly, we reveal that depletion of RIF1 accelerates 53BP1 repositioning. This observation supports a model that RIF1 regulates the 53BP1 barrier. The rapid repositioning in the absence of RIF1 may accelerate the speed and/or length of resection at DSBs undergoing HR. 53BP1 forms oligomers and the tudor domains of 53BP1 bind the histone H4 K20me2 (Zimmermann and de Lange, 2014). The role of 53BP1 may be to stabilize the chromatin structure in close proximity to DSB sites to limit access by nucleases. Indeed, depletion of BRCA1 or PP4C, which impede 53BP1 repositioning, reduced EXO1 recruitment at DNA damage sites. This supports the notion that the 53BP1 barrier limits the access of nucleases to prevent extensive resection until the repair pathway is directed toward HR. Additionally, PTIP has been reported to regulate resection, and it is possible that a similar mechanism of phosphorylation/dephosphorylation regulates its recruitment. Our data do not exclude this possibility, but analysis of 7A/6A mutants shows clearly that 53BP1-T543 undergoes phosphorylation and must be dephosphorylated to allow RIF1 release and the progression of HR.

A previous study has shown that PP4C also dephosphorylates pT1609 and pS1618 of 53BP1 to allow the recruitment of 53BP1 to chromatin in G_1 phase (Lee et al., 2014). PP4C also dephosphorylates other damage response proteins, e.g., RPA and H2AX, in response to DNA damage (Chowdhury et al., 2008; Lee et al., 2010; Nakada et al., 2008). Thus, PP4C is one of the important phosphatases to facilitate DNA damage responses including HR. Phosphatase specificity for targets is regulated by multiple factors, including regulatory subunits. In this study, we identified the requirement of PP4R2 for RIF1 release. We identified IR-induced PLA signals between BRCA1-PP4C and between 53BP1-PP4C, supporting the notion that BRCA1 participates in the process of 53BP1 dephosphorylation by PP4C. However, BRCA1 depletion does not affect 53BP1-PP4C interaction nor

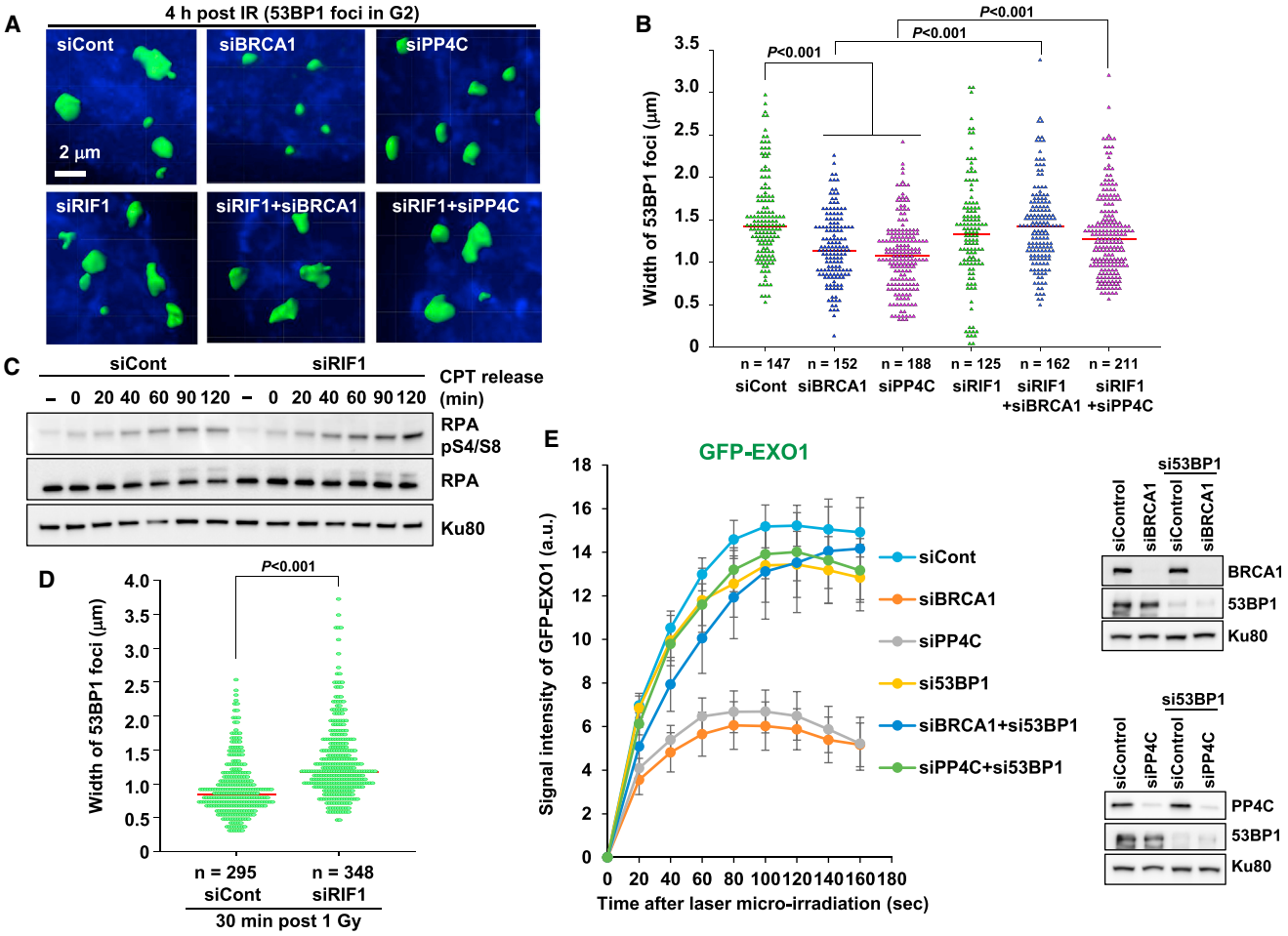

Figure 6. RIF1 Maintains the 53BP1 Barrier by Preventing 53BP1 Repositioning

(A) Representative images of 53BP1 foci enlargement in BRCA1- or PP4C-depleted cells ± siRIF1 are shown. The original images are shown in Figure S6A.

(B) Defective 53BP1 foci enlargement in BRCA1- or PP4C-depeleted cells was rescued by RIF1 siRNA. 53BP1 foci enlargement in 1BR (WT) hTERT G_2 cells was examined 4 hr after irradiation with 1 Gy. Knockdown efficiencies are shown in Figures S6B–S6D.

(C) Depletion of RIF1 accelerates timing of resection. Resection was examined by RPA-pS4/8 in A549 cells following treatment with 2 μM CPT.

(D) Depletion of RIF1 causes rapid 53BP1 foci enlargement in cells in G_2. 53BP1 foci were examined in 1BR (WT) hTERT cells 30 min after exposure to 1 Gy. Representative images are shown in Figure S6E.

(E) Impaired EXO1 recruitment in BRCA1- or PP4C-depleted cells is alleviated by 53BP1 depletion. Localized DNA damage was induced by laser irradiation in U2OS cells expressing GFP-tagged EXO1 and mKO-tagged Geminin following Control, BRCA1, or PP4C siRNA with or without 53BP1 siRNA treatment. Representative images up to 160 s post-laser irradiation are shown in Figure S7. GFP signal intensity was monitored and quantified for 160 s post-irradiation. Knockdown efficiency is shown in the right panel.

In (B)–(E), a similar result is obtained with more than two independent experiments. The p values were derived from Student's two-tailed t test or Mann-Whitney U test.

PP4C recruitment to damage sites. Thus, BRCA1 does not appear to directly mediate PP4C recruitment; rather, its function appears to be indirect, for example, by recruiting further PP4C regulatory subunits or an environment allowing PP4C to dephosphorylate 53BP1. In addition to PP4C, we found that PP1CB also contributes to dephosphorylation of 53BP1-pT543 and RIF1 loss, although the impact on pT543 foci loss is modest. Because PP1C knockdown was not additive with PP4C knockdown, it is possible that PP1C has a distinct role in determining RIF1 release. The analysis of RIF1 in 7A, 6A (T543 is WT), and T543A (6WT) mutant supports the notion that PP4C has a major role in dephosphorylation of the seven S/TQ sites (six S/TQ plus T543). However, the contribution of other phosphatases cannot be excluded. Although we observed no redundancy between PP4C and PP1CB, further studies are required to define the role played by PP1CB. A recent report showed that RIF1 is polyubiquitinated by UHRF1 in a BRCA1-dependent manner, raising the possibility that BRCA1 could have a role via posttranslational modification (Zhang et al., 2016). This report proposes a further model that dephosphorylation of 53BP1 by phosphatases may be required to phosphorylate UHRF1, followed by RIF1 ubiquitination and subsequent RIF1 release. Whether RIF1 ubiquitination

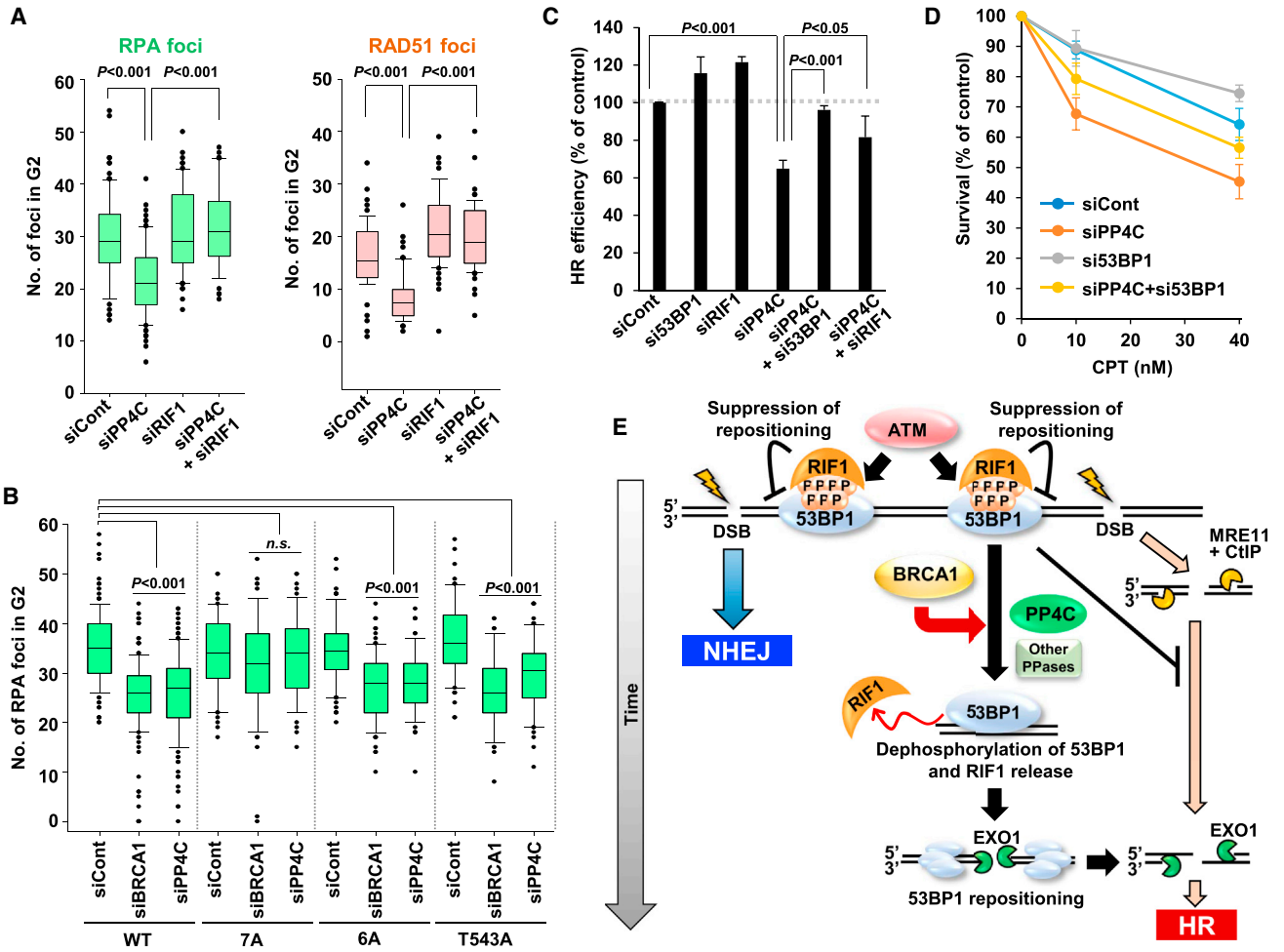

Figure 7. PP4C Promotes DNA-End Resection and HR in the 53BP1-BRCA1 Axis

(A) Depletion of PP4C reduces IR-induced RPA/RAD51 foci formation in cells in G_2. The defect is rescued by depletion of RIF1. RPA/RAD51 foci in A549 cells were examined 2 hr after irradiation with 1 Gy.

(B) Analysis of RPA foci formation in 53BP1 phosphor mutants. RPA foci at 2 hr post 1 Gy was examined in A549 cells expressing siRNA-resistant FLAG-53BP1 WT, 7A, 6A, or T543A mutants with or without Control, BRCA1, or PP4C siRNA.

(C) HR deficiency in PP4C-depeleted cells is rescued by RIF1 or 53BP1 deficiency. DR-GFP U2OS cells were transfected with 53BP1, RIF1, and/or PP4C siRNAs. The fraction of GFP-positive cells was measured by FACS.

(D) PP4C-depleted cells after CPT treatment exhibit hypersensitivity compared to control cells. Depletion of 53BP1 rescues this hypersensitivity in PP4C-depleted cells. The sensitivity in U2OS cells transfected with PP4C with or without 53BP1 siRNAs was examined by colony formation assay.

(E) A model for the role of BRCA1 in promoting DNA-end resection in control cells. Following the induction of DSBs, ATM phosphorylates 53BP1, even in S/G_2 phase, at all the DSB sites followed by the transient recruitment of RIF1, which generates a pro-NHEJ environment. In G_2, NHEJ factors rapidly repair ~70% of the DSBs. The remaining DSBs are not excessively resected due to the 53BP1 barrier in the presence of RIF1 from ~0.5–1 hr post-IR. MRE11 endonuclease initiates resection. When timely repair by NHEJ does not ensue, BRCA1 promotes 53BP1 dephosphorylation. PP4C plays a major role in 53BP1 dephosphorylation, which promotes RIF1 release. However, a contribution of other phosphatases cannot be excluded. Although BRCA1-PP4C interact, the function of BRCA1 is not simply to recruit PP4C. As resection proceeds, ATM activity is diminished. Thus, the failure to rephosphorylate 53BP1 combined with its dephosphorylation results in the release of RIF1. Removal of RIF1 allows 53BP1 repositioning. After removing the 53BP1 barrier, EXO1 can progress the elongation of resection required for HR.

Values in (C) and (D) are means ± SEM from three independent experiments. In (A) and (B), a similar result is obtained with more than two independent experiments. The p values were derived from Student's two-tailed t test or Mann-Whitney U test.

occurs prior to or after dephosphorylation remains to be determined. Alternatively, BRCA1 may promote SMARCAD1-dependent chromatin remodeling to aid 53BP1/PP4C interaction for 53BP1 dephosphorylation (Densham et al., 2016).

There is mounting evidence that, even in S/G_2, NHEJ makes the first attempt to repair DSBs prior to a switch to HR (Chanut et al., 2016; Shibata et al., 2011, 2014). Here, we propose that ATM is initially activated at unresected DSBs, i.e., at all the DSB ends in G_2 phase causing RIF1 recruitment. At this early stage, either BRCA1-PP4C is not functional or robust ATM activity out-competes PP4C activity. If timely repair by NHEJ does not ensue, then resection is initiated, promoting the switch to ATR signaling,

which does not phosphorylate 53BP1 for RIF1 recruitment. However, BRCA1 plays a critical role in regulating RIF1 release via aiding the dephosphorylation of 53BP1 by PP4C. Collectively, we demonstrate that 53BP1 dephosphorylation by BRCA1-PP4C promotes the repair pathway switch toward HR in S/G_2 after transient 53BP1 phosphorylation and RIF1 recruitment (Figure 7E). Although the pathway choice between NHEJ and HR has been discussed by regulation of cell-cycle phase, the findings in this study help to understand how the repair pathway switch from NHEJ to HR is coordinated by BRCA1 in S/G_2 phase.

EXPERIMENTAL PROCEDURES

Cell Culture and Irradiation

1BR human fibroblasts (WT) hTERT cells were cultured in the Alpha modification of minimum essential medium (MEM) with 10% fetal calf serum (FCS). A549 and U2OS cells were cultured in MEM with 10% FCS. The procedure of irradiation, drug treatment, and siRNA/vector transfection are described in Supplemental Experimental Procedures.

Analysis of Immunofluorescence Images

The procedure of immunofluorescence staining and immunoblotting are described in Supplemental Experimental Procedures (Shibata et al., 2011). Microscopic images were taken by an Applied Precision DeltaVision OMX microscope with a 60× objective. Z stacks were taken over 2- to 3-μm areas (sections taken every 0.25 μm), and individual nuclei were imaged. Deconvolution was performed by softWoRx software. 3D images of 53BP1 foci were obtained by using the Applied Precision DeltaVision OMX microscope, and the maximal 53BP1 width was measured following polygon rendering by Imaris 8.2.1. Boxplots were constructed with SigmaPlot 12.0 with 100–200 foci from at least two independent experiments. Scoring of IR-induced foci and statistical analysis are described in Supplemental Experimental Procedures.

Quantification of 53BP1-pT543 Using Fluorescence-Activated Cell Sorting

Cells were irradiated 48 hr post-siRNA transfection. Irradiated cells were trypsinized and washed three times, and suspended cells were fixed with 3% PFA-2% sucrose, followed by permeabilization of cells with 0.2% Triton in PBS for 2.5 min. Cells were incubated with primary 53BP1-pT543 rabbit antibody, followed by Alexa Fluor 488-conjugated secondary antibody. Cells were then washed and resuspended in propidium iodide (PI) with RNase A (Sigma-Aldrich). Cells were analyzed using a fluorescence-activated cell sorter (Attune NxT Cytometer). S/G_2 cells were identified based on DNA content as assessed by PI staining.

EXO1 Laser Experiment

U2OS cells expressing green fluorescence protein (GFP)-tagged EXO1 and mKusabira-Orange2 (KO2)-tagged Geminin were transfected with Control, BRCA1, or PP4C siRNA. Following siRNA transfection, cells were seeded on glass-bottom dishes (Matsunami) and incubated in the presence of 10 μM BrdU (Sigma) until the laser experiment. Geminin-positive S/G_2 cells were irradiated with 405-nm UV laser using the TURF mode in the Applied Precision DeltaVision OMX microscope. GFP signal was monitored through 60× objective lens every 20 s up to 160 s post-laser irradiation. The signal intensity was quantified with ImageJ software.

HR Assay

Direct repeat (DR)-GFP U2OS (3×10^5 cells) were transfected with siRNAs using HiPerFect transfection reagent (QIAGEN). After 24 hr, cells were trypsinized and transfected with siRNAs again and plated into 60-mm dishes. At 24 hr after the second siRNA transfection, either EGFP-empty or I-*Sce*I vector was transfected by Lipofectamine 3000 (Thermo Fisher Scientific). Medium was refreshed 3 hr after transfection. GFP-positive cells were measured by Attune acoustic focusing cytometer (Thermo Fisher Scientific) at 48 hr after the I-*Sce*I transfection.

Survival Analysis

At 48 hr after siRNA transfection, U2OS cells were reseeded and allowed to adhere for 12 hr before treatment with 10 or 40 nM CPT for 1 hr. The cells were then washed three times with PBS, and fresh medium was added. Cells were incubated for 10 days at 37°C to allow colony formation. Colonies were fixed with 2% PFA, and then stained with 0.3% crystal violet in PBS and counted. The results were normalized to the plating efficiencies.

Scoring of IR-Induced Foci and Statistical Analysis

Foci scoring was carried out blindly with >30 cells/samples or 800 foci/sample being scored (Shibata et al., 2011). Unless stated otherwise, all foci analyses represent the mean and SD of three experiments. To examine IR-induced foci in G_2 cells, 4 μM aphidicolin (APH) was added after irradiation. APH alone does not affect DSB repair kinetics in G_2 and G_1 cells (Shibata et al., 2011). APH was added immediately after IR to block S-to-G_2 progression and to enhance pan-nuclear signals due to replication stress in S phase. All data were derived from three to four independent experiments unless stated otherwise. Boxplots and dot density plots from >100 samples were created by SigmaPlot 12.0. Statistical significance was determined using Student's two-tailed t test or Mann-Whitney U test by SigmaPlot 12.0.

SUPPLEMENTAL INFORMATION

Supplemental Information includes Supplemental Experimental Procedures, seven figures, and three tables and can be found with this article online at http://dx.doi.org/10.1016/j.celrep.2016.12.042.

AUTHOR CONTRIBUTIONS

M.I. and A.S. designed the experiments, analyzed the data, and wrote the paper. M.I., A.N., Y.H., R.S., and A.S. performed the experiments. Acquired data were analyzed and interpreted by M.I., A.N., and A.S. All foci analysis was performed by M.I. and A.S. Western blot was performed by M.I., Y.H., and A.S. FACS analysis, including 53BP1 pT543 analysis and DR-GFP, was performed by M.I. and A.S. PLA analysis was performed by M.I. 53BP1 foci enlargement was analyzed by M.I., R.S., and A.S. The clonogenic survival experiment was performed by A.N. Representative images were taken by M.I., R.S., and A.S. MRE11 inhibitors were synthesized by E.P. U2OS GFP-EXO1 cell line was established by R.N. Protein phosphatase siRNA library was designed and provided by S.N. The manuscript was reviewed by S.N. Crucial advice about the role of protein phosphatases was provided by S.N. siRNA-resistant 53BP1 vectors were made by S.-Y.I. and C.O. Administrative, technical, or material support was provided by T.O., H.S., Y.Y., and T.N. The study was supervised by A.S.

ACKNOWLEDGMENTS

We greatly appreciate support from and fruitful discussion with Penny A. Jeggo during editing of the manuscript. We thank Ryo Sakasai for their helpful discussions. We thank Yoshimi Omi, Yoko Hayashi, Shiho Nakanishi, and Yuka Kimura for their assistance with laboratory work. This study was supported by the Takeda Science Foundation, the Suzuken Memorial Foundation, the Uehara Memorial Foundation, Mochida Memorial Foundation for Medical and Pharmaceutical Research, Kowa Life Science Foundation, the Sumitomo Foundation and JSPS KAKENHI Grants JP26701005 and JP26670549 (to A.S.), JP26241014 (to S.N.), JP15H02816 (to A.N.), JP20114006 and JP25116004 (to C.O.), and JP16H05888 (to R.N.).

Received: March 4, 2016
Revised: October 3, 2016
Accepted: December 13, 2016
Published: January 10, 2017

REFERENCES

Arnaudeau, C., Lundin, C., and Helleday, T. (2001). DNA double-strand breaks associated with replication forks are predominantly repaired by homologous

recombination involving an exchange mechanism in mammalian cells. J. Mol. Biol. *307*, 1235–1245.

Bouwman, P., Aly, A., Escandell, J.M., Pieterse, M., Bartkova, J., van der Gulden, H., Hiddingh, S., Thanasoula, M., Kulkarni, A., Yang, Q., et al. (2010). 53BP1 loss rescues BRCA1 deficiency and is associated with triple-negative and BRCA-mutated breast cancers. Nat. Struct. Mol. Biol. *17*, 688–695.

Broderick, R., Nieminuszczy, J., Baddock, H.T., Deshpande, R.A., Gileadi, O., Paull, T.T., McHugh, P.J., and Niedzwiedz, W. (2016). EXD2 promotes homologous recombination by facilitating DNA end resection. Nat. Cell Biol. *18*, 271–280.

Bunting, S.F., Callén, E., Wong, N., Chen, H.T., Polato, F., Gunn, A., Bothmer, A., Feldhahn, N., Fernandez-Capetillo, O., Cao, L., et al. (2010). 53BP1 inhibits homologous recombination in Brca1-deficient cells by blocking resection of DNA breaks. Cell *141*, 243–254.

Callen, E., Di Virgilio, M., Kruhlak, M.J., Nieto-Soler, M., Wong, N., Chen, H.T., Faryabi, R.B., Polato, F., Santos, M., Starnes, L.M., et al. (2013). 53BP1 mediates productive and mutagenic DNA repair through distinct phosphoprotein interactions. Cell *153*, 1266–1280.

Chanut, P., Britton, S., Coates, J., Jackson, S.P., and Calsou, P. (2016). Coordinated nuclease activities counteract Ku at single-ended DNA double-strand breaks. Nat. Commun. *7*, 12889.

Chapman, J.R., Sossick, A.J., Boulton, S.J., and Jackson, S.P. (2012a). BRCA1-associated exclusion of 53BP1 from DNA damage sites underlies temporal control of DNA repair. J. Cell Sci. *125*, 3529–3534.

Chapman, J.R., Taylor, M.R., and Boulton, S.J. (2012b). Playing the end game: DNA double-strand break repair pathway choice. Mol. Cell *47*, 497–510.

Chapman, J.R., Barral, P., Vannier, J.B., Borel, V., Steger, M., Tomas-Loba, A., Sartori, A.A., Adams, I.R., Batista, F.D., and Boulton, S.J. (2013). RIF1 is essential for 53BP1-dependent nonhomologous end joining and suppression of DNA double-strand break resection. Mol. Cell *49*, 858–871.

Chowdhury, D., Xu, X., Zhong, X., Ahmed, F., Zhong, J., Liao, J., Dykxhoorn, D.M., Weinstock, D.M., Pfeifer, G.P., and Lieberman, J. (2008). A PP4-phosphatase complex dephosphorylates gamma-H2AX generated during DNA replication. Mol. Cell *31*, 33–46.

Davé, A., Cooley, C., Garg, M., and Bianchi, A. (2014). Protein phosphatase 1 recruitment by Rif1 regulates DNA replication origin firing by counteracting DDK activity. Cell Rep. *7*, 53–61.

Densham, R.M., Garvin, A.J., Stone, H.R., Strachan, J., Baldock, R.A., Daza-Martin, M., Fletcher, A., Blair-Reid, S., Beesley, J., Johal, B., et al. (2016). Human BRCA1-BARD1 ubiquitin ligase activity counteracts chromatin barriers to DNA resection. Nat. Struct. Mol. Biol. *23*, 647–655.

Escribano-Díaz, C., Orthwein, A., Fradet-Turcotte, A., Xing, M., Young, J.T., Tkáč, J., Cook, M.A., Rosebrock, A.P., Munro, M., Canny, M.D., et al. (2013). A cell cycle-dependent regulatory circuit composed of 53BP1-RIF1 and BRCA1-CtIP controls DNA repair pathway choice. Mol. Cell *49*, 872–883.

Feng, L., Fong, K.W., Wang, J., Wang, W., and Chen, J. (2013). RIF1 counteracts BRCA1-mediated end resection during DNA repair. J. Biol. Chem. *288*, 11135–11143.

Garcia, V., Phelps, S.E., Gray, S., and Neale, M.J. (2011). Bidirectional resection of DNA double-strand breaks by Mre11 and Exo1. Nature *479*, 241–244.

Huen, M.S., Sy, S.M., and Chen, J. (2010). BRCA1 and its toolbox for the maintenance of genome integrity. Nat. Rev. Mol. Cell Biol. *11*, 138–148.

Jeggo, P.A., and Löbrich, M. (2006). Contribution of DNA repair and cell cycle checkpoint arrest to the maintenance of genomic stability. DNA Repair (Amst.) *5*, 1192–1198.

Jeggo, P.A., Geuting, V., and Lobrich, M. (2011). The role of homologous recombination in radiation-induced double-strand break repair. Radiother. Oncol *101*, 7–12.

Kakarougkas, A., Ismail, A., Katsuki, Y., Freire, R., Shibata, A., and Jeggo, P.A. (2013). Co-operation of BRCA1 and POH1 relieves the barriers posed by 53BP1 and RAP80 to resection. Nucleic Acids Res. *41*, 10298–10311.

Lee, D.H., Pan, Y., Kanner, S., Sung, P., Borowiec, J.A., and Chowdhury, D. (2010). A PP4 phosphatase complex dephosphorylates RPA2 to facilitate DNA repair via homologous recombination. Nat. Struct. Mol. Biol. *17*, 365–372.

Lee, D.H., Goodarzi, A.A., Adelmant, G.O., Pan, Y., Jeggo, P.A., Marto, J.A., and Chowdhury, D. (2012). Phosphoproteomic analysis reveals that PP4 dephosphorylates KAP-1 impacting the DNA damage response. EMBO J. *31*, 2403–2415.

Lee, D.H., Acharya, S.S., Kwon, M., Drane, P., Guan, Y., Adelmant, G., Kalev, P., Shah, J., Pellman, D., Marto, J.A., and Chowdhury, D. (2014). Dephosphorylation enables the recruitment of 53BP1 to double-strand DNA breaks. Mol. Cell *54*, 512–525.

Nakada, S., Chen, G.I., Gingras, A.C., and Durocher, D. (2008). PP4 is a gamma H2AX phosphatase required for recovery from the DNA damage checkpoint. EMBO Rep. *9*, 1019–1026.

Panier, S., and Boulton, S.J. (2014). Double-strand break repair: 53BP1 comes into focus. Nat. Rev. Mol. Cell Biol. *15*, 7–18.

Sartori, A.A., Lukas, C., Coates, J., Mistrik, M., Fu, S., Bartek, J., Baer, R., Lukas, J., and Jackson, S.P. (2007). Human CtIP promotes DNA end resection. Nature *450*, 509–514.

Schlegel, B.P., Jodelka, F.M., and Nunez, R. (2006). BRCA1 promotes induction of ssDNA by ionizing radiation. Cancer Res. *66*, 5181–5189.

Shibata, A., Conrad, S., Birraux, J., Geuting, V., Barton, O., Ismail, A., Kakarougkas, A., Meek, K., Taucher-Scholz, G., Löbrich, M., and Jeggo, P.A. (2011). Factors determining DNA double-strand break repair pathway choice in G_2 phase. EMBO J. *30*, 1079–1092.

Shibata, A., Moiani, D., Arvai, A.S., Perry, J., Harding, S.M., Genois, M.M., Maity, R., van Rossum-Fikkert, S., Kertokalio, A., Romoli, F., et al. (2014). DNA double-strand break repair pathway choice is directed by distinct MRE11 nuclease activities. Mol. Cell *53*, 7–18.

Shiotani, B., and Zou, L. (2009). Single-stranded DNA orchestrates an ATM-to-ATR switch at DNA breaks. Mol. Cell *33*, 547–558.

Söderberg, O., Gullberg, M., Jarvius, M., Ridderstråle, K., Leuchowius, K.J., Jarvius, J., Wester, K., Hydbring, P., Bahram, F., Larsson, L.G., and Landegren, U. (2006). Direct observation of individual endogenous protein complexes in situ by proximity ligation. Nat. Methods *3*, 995–1000.

Stiff, T., O'Driscoll, M., Rief, N., Iwabuchi, K., Löbrich, M., and Jeggo, P.A. (2004). ATM and DNA-PK function redundantly to phosphorylate H2AX after exposure to ionizing radiation. Cancer Res. *64*, 2390–2396.

Symington, L.S., and Gautier, J. (2011). Double-strand break end resection and repair pathway choice. Annu. Rev. Genet. *45*, 247–271.

Venkitaraman, A.R. (2004). Tracing the network connecting BRCA and Fanconi anaemia proteins. Nat. Rev. Cancer *4*, 266–276.

Zhang, H., Liu, H., Chen, Y., Yang, X., Wang, P., Liu, T., Deng, M., Qin, B., Correia, C., Lee, S., et al. (2016). A cell cycle-dependent BRCA1-UHRF1 cascade regulates DNA double-strand break repair pathway choice. Nat. Commun. *7*, 10201.

Zhu, Z., Chung, W.H., Shim, E.Y., Lee, S.E., and Ira, G. (2008). Sgs1 helicase and two nucleases Dna2 and Exo1 resect DNA double-strand break ends. Cell *134*, 981–994.

Zimmermann, M., and de Lange, T. (2014). 53BP1: pro choice in DNA repair. Trends Cell Biol. *24*, 108–117.

Zimmermann, M., Lottersberger, F., Buonomo, S.B., Sfeir, A., and de Lange, T. (2013). 53BP1 regulates DSB repair using Rif1 to control 5′ end resection. Science *339*, 700–704.